WARSAW UNIVERSITY OF TECHNOLOGY Index 351733
FACULTY OF CIVIL ENGINEERING
COMMITTEE FOR CIVIL AND WATER ENGINEERING
POLISH ACADEMY OF SCIENCES ISSN 1230-2945

DOI: 10.24425/ace.2026.157483

ARCHIVES OF CIVIL ENGINEERING

Vol. LXXII ISSUE 1 2026

pp. 421 –434

Research paper

Experimental investigation of vertical bearing capacity and group pile effect for combined long and short pile foundations in Loess

Tianzhong Ma[1], Mengli Tian[2], Zhengzhen Wang[3]

Abstract: To simultaneously meet both bearing capacity and settlement requirements in loess areas, the introduction of novel pile foundation types is crucial. A large-scale indoor model experimental was designed and conducted. The experiment tested four variables: pile spacing, pile type, number of piles, and pile length. A comprehensive analysis was conducted to determine the vertical bearing capacity of combined long and short pile foundations, including the influence of the group pile effect on combined long and short pile foundation performance. The experimental results reveal that the lateral frictional resistance of both long and short piles in the combined long and short pile foundations system acted in an alternating manner. Furthermore, the axial force and lateral frictional resistance of the corner piles were slightly greater than those of the edge and center piles. Increasing the pile spacing, the group pile effect coefficient increases from 0.83 to 0.95. This results in a 16.7% enhancement in the bearing capacity of the group pile foundation. Modifying the pile type increases the group pile effect coefficient from 0.825 to 0.94. This leads to a roughly 16% improvement in bearing capacity compared to the ring-shaped pile configuration. Reducing the number of long piles, the group effect coefficient increased from 0.825 to 0.80. The overall ultimate bearing capacity decreases by approximately 20%. Increasing the pile length results in a group pile effect coefficient of 0.87, representing a 0.45 increase compared to the base pile configuration. Consequently, the bearing capacity of the group pile foundation improves by 18.1%.

Keywords: combined long and short pile foundation, loess, vertical bearing capacity, pile group effect, model experimental

[1]Associate Prof, PhD., Eng., Lanzhou University of Technology, School of Civil Engineering, No. 287 Langongping Road, Lanzhou, China, e-mail: matz0914@163.com, ORCID: 0000-0003-0707-1058
[2]MSc., Lanzhou University of Technology, School of Civil Engineering, No. 287 Langongping Road, Lanzhou, China, e-mail: tianmengli2022@163.com, ORCID: 0009-0007-7645-0605
[3]Associate Prof, PhD., Eng., Lanzhou University of Technology, School of Civil Engineering, No. 287 Langongping Road, Lanzhou, China, e-mail: wangzz@lut.edu.cn, ORCID: 0000-0001-8470-1258

1. Introduction

The Loess area is characterized by unique geological conditions, with soil layers exhibiting high moisture content and plasticity, making them susceptible to settlement and deformation [1]. The construction of building foundations in such regions presents significant challenges. The susceptibility of loess to wetting-induced collapse and a significant reduction in bearing capacity upon water saturation poses a major concern [2]. As a result, the design concept of combined long and short pile foundations has emerged as a viable alternative. The combined long and short pile foundation is also known as a "settlement reduction pile". By combining the characteristics of long and short piles, this approach aims to control foundation settlement and enhance bearing capacity [3]. The short piles primarily contribute to load-bearing capacity, effectively supporting a significant portion of the applied load. In contrast, long piles play a crucial role in controlling foundation settlement by increasing the number and distribution of piles to distribute the load evenly [4]. There is a lack of research on the use of long and short pile foundations in loess areas, making it an area that warrants further investigation.

In recent years, there has been a significant amount of research conducted by scholars on combined long and short pile foundations, yielding fruitful results. Su-Hyung Lee et al [5] investigated the influence of varying pile spacing on pile-soil-pile and cap-pile-soil interactions through model experiments conducted on single piles and pile groups. Zhang et al. [6] proposed a simplified hyperbolic model for nonlinear load-displacement analysis of pile groups in multi-layered soil, accounting for pile-pile interaction effects on unit skin friction. Li and Gong et al [7] proposed a combined load transfer and shear displacement method for predicting the bearing capacity for both new and existing pile groups. Li et al [8] investigated the bearing characteristics of pile foundations in different soil layers by adjusting the pile length, diameter, and spacing. Gao et al [9] investigated the load-bearing behavior of combined long and short pile foundations in loess regions through field testing on a high-speed railway foundation. Li et al [10] conducted indoor model experiments to examine the impact of varying pile length ratios and spacing on the load-bearing behavior of combined long and short pile foundations in loess areas. Building upon the shear displacement model proposed by Randolph and Wroth [11] Shi et al [12] investigated the impact of the "curtain and reinforcement" effect of pile groups on their load-bearing capacity and settlement. Ma et al [13] developed a method for calculating the neutral point of foundation piles based on theoretical analysis and model testing. Xiao Y et al [14] proposed a method for calculating the stress and settlement of the subgrade under a composite soft-hard pile foundation, based on the Boussinesq and Mindlin solutions. Shalabi F et al [15] employed numerical simulations to examine how the length-diameter ratio of the pile impacts both the deformation of the pile itself and its perimeter under load. Bhaduri et al [16] proposed a new finite element method for analyzing the behavior of a flexible composite pile raft foundation located in layered soil within a displacement-based framework. Bernardes et al. [17] monitored strain in columns and piles, raft-soil interface stress, and foundation settlement to analyze a high-rise building's pile raft foundation. Koichiro et al [18] demonstrated that the load-bearing capacity of pile groups is influenced by group effects. Kong et al [19] investigated the variation patterns of the group effect coefficient through an indoor model experiment.

Numerous studies have been conducted on the application of pile group foundations, yet research into the combined use of long and short piles remains limited. To address this limitation, this study aims to investigate the load transfer characteristics of combined long and short pile foundations in loess areas, as well as the impact of group pile effects on bearing capacity, through large-scale model experimental.

2. Experiment scheme

2.1. Indoor model experimental scheme design

A total of sixteen experimental piles are included in the experiment, divided into four sets of control experimental: varying pile length, spacing, number, and type. These variations are designed to investigate the bearing capacity and group pile effect of combined long and short pile foundations in loess areas. The experimental scheme is presented in Table 1.

The pile arrangement for the varying pile length and varying pile spacing (4D) conditions is identical, as depicted in Fig. 1(a). Fig. 1(b) presents the pile arrangement for the varying pile spacing (6D) condition. The pile arrangement for the varying pile number condition (4 long and 8 short piles) is shown in Fig. 1(c). Fig. 1(d) illustrates the pile arrangement for the varying pile type conditions (triangular pattern).

Table 1. Pile body layout diagram for various working conditions (unit: mm): blue – short pile; red – long pile

Trial classification	**Experimental groups**	**Pile diameter D (mm)**	**Pile spacing**	**Length of short piles (mm)**	**Length of long piles (mm)**	**Number of short piles $n1$**	**Number of long piles $n2$**
Varying pile length	1–1#	60	4D	600	1200	8	8
	1–2#	60	4D	600	1400	8	8
Varying pile spacing	2–1#	60	4D	600	1200	8	8
	2–2#	60	6D	600	1200	8	8
Varying the number of piles	3–1#	60	4D	600	1200	8	8
	3–2#	60	4D	600	1200	12	4
Varying the arrangement shape of piles	Ring-like pile type	60	4D	600	1200	8	8
	Plum blossom shape pile	60	4D	600	1200	8	8

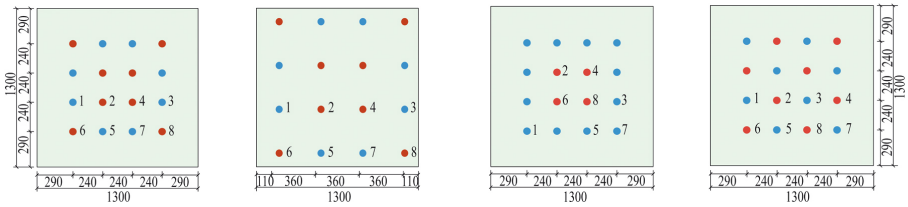

Fig. 1. Pile body layout diagram for various working conditions (unit: mm): blue – short pile; red – long pile

2.2. Design and fabrication of the model apparatus

2.2.1. Model box

The model box, measuring 2.1 × 2.1 × 1.8 m, is constructed with 15 mm thick tempered glass on all four sides (Fig. 2). This allows for clear observation of soil fill height variations during compaction and pile settlement throughout the experiment. A sturdy frame is constructed from steel pipes and angle irons welded together to form the outer perimeter of the box. The box bottom is fabricated by welding a 5 mm steel plate to the lower steel pipes.

2.2.2. Loading frame

The experimental loading device utilizes a custom-built horizontal-vertical loading frame. The frame comprises vertical and horizontal reaction beams, I-beam supports (supporting the model box), and I-beam support ribs. The loading frame's upper and lower crossbeams were 2.6 meters in length, and the frame's height was 2.2 meters. All of the six support beams at the bottom of the loading rack are 1.3 m in length. A schematic diagram of the loading frame is shown in Fig. 2.

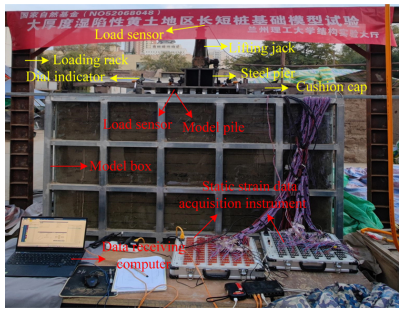

Fig. 2. Model box diagram

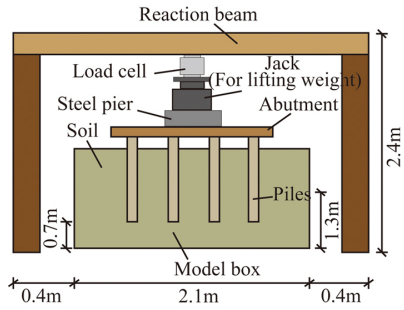

Fig. 3. Diagram of the loading device

2.2.3. Loading device

Vertical forces are applied to the vertical beam of the custom-built loading frame by a 20T hydraulic jack, coupled with a 40 × 40 × 40 cm square steel block. The jack is elevated and force is transferred to the supporting platform by the steel block. A 20T load cell is positioned above the jack to monitor the applied force. The loading device is illustrated in Fig. 3.

2.2.4. Model piles

Adherence to the principles of model experimental similarity dictated the use of hollow aluminum pipe piles, with an outer diameter of 60 mm and a wall thickness of 1.5 mm, as model piles. Long piles and short piles all with a uniform diameter. A custom-designed aluminum cap sealed the base of each pile. Both the pile caps and pile bodies were fabricated from aluminum tubing possessing a stiffness of 59.7 GPa.

2.2.5. Data acquisition system

For pile shaft stress measurement, strain gauges, a DH3816N static strain data acquisition instrument, a stabilized power supply, and a computer were employed. Bearing platform settlement was measured using six 20 mm electronic dial gauges with a precision of 0.01 mm.

3. Experimental methods and procedures

3.1. Production of model piles

The hollow aluminum pipe was first polished smooth on the exterior. Epoxy resin glue was then applied, followed by a coating of fine sand that had been passed through a 3mm sieve. This roughening process was conducted to simulate the surface condition of actual piles in real-world engineering projects, as illustrated in Fig. 4.

3.2. Strain gauge placement

The strain gauge model is BFH120-3AA-R-D150 with 120Ω resistance and 2.0±1% sensitivity factor. The strain gauges are arranged symmetrically on both sides of the aluminum tube concerning the corresponding cross-section, and the arrangement is shown in Fig. 4.

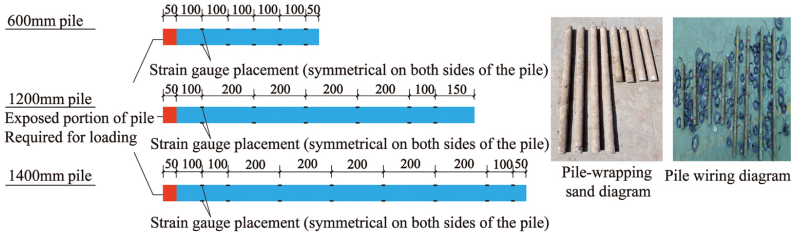

Fig. 4. Schematic diagram of the arrangement of the strain gauge (unit: mm)

3.3. Model pile placement

The soil used in this experiment was collapsible loess from the northwest region. The preparation of the surrounding soil involves crushing, sieving, and moistening processes to achieve the desired soil properties. The experiment measured a moisture content of 14.1% in the soil. The compaction degree was measured to be 0.91 after the backfill was completed. The specific process is as follows:

Before filling, the soil was pre-wetted by adding the calculated amount of water and allowing it to soak for 24 hours. The soil was then backfilled into the box in layers. The soil was filled in 100 mm layers, ensuring a consistent drop height for each layer to maintain uniform soil compaction. After each layer was filled, the surface was leveled to half the layer thickness and compacted. A custom-designed horizontal loading frame and leveling ruler were used to accurately position the piles. This process is illustrated in Fig. 5.

3.4. Loading and measuring process

A pile-top force transmission method was employed for the experimental loading. A 2 cm thick steel plate served as the loading plate, and a 10T load cell was placed atop each pile to measure vertical load. A separate 20T load cell was installed on the jack to measure the total applied load. The experimental model pile's bearing capacity was estimated based on the Technical Specification for Building Pile Foundation (JGJ94-2008) [20] and loaded incrementally at 7 kN per stage until failure. Data acquisition was performed using a DH3816N static strain data collector. The loading measurement process is illustrated in Fig. 2. Rather Fig. 5?

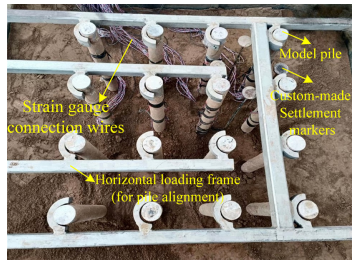

Fig. 5. Pile positioning

4. Experimental results and analysis

The ultimate bearing capacity of 0.6 m, 1.2 m, and 1.4 m piles was determined to be 3.5 kN, 6.5 kN, and 7 kN, respectively, by single pile tests. In this paper, the bearing capacity of short and long piles is obtained by analyzing the force of side piles, center piles, and corner piles in short and long piles and according to the symmetry of piles, and the results of the bearing capacity of piles and effect coefficients of piles for each working condition are compared and analyzed. The group pile effect coefficient is determined using the method outlined in the "Pile Foundation Engineering Manual" [21].

4.1. Analysis of variable pile spacing experimental results

An experiment was conducted with a pile spacing of 4D, employing 8 long piles and 8 short piles. Fig. 6 presents the axial force distribution curves for the 16 group piles under vertical loading. The foundation piles exhibited varying bearing capacities, influenced by their distinct locations within the pile group. Notably, corner piles demonstrated a higher bearing capacity compared to center piles. The loads on the center pile, corner pile, and variable pile

are 5.75 kN, 6 kN, and 2.6 kN, respectively. Despite variations in load distribution, even at failure, the center and side piles did not reach the ultimate bearing capacity achieved by the corner piles. An ultimate bearing capacity of 66 kN was observed for both long and short piles at failure, resulting in a calculated group pile effect of 0.825.

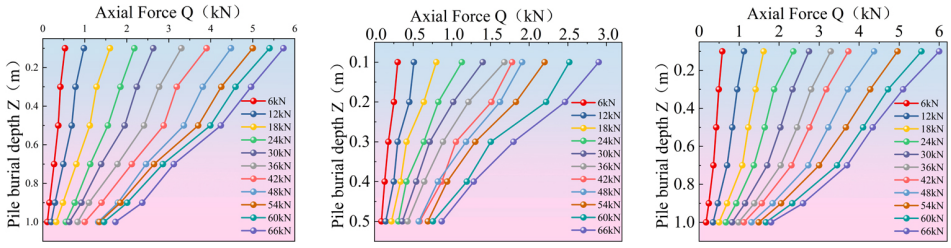

Fig. 6. Axial force of the pile under 4*D* working conditions: (a) 4# Center pile (long pile); (b) 7# Side pile (short pile); (c) 8# Corner pile (long pile)

Lateral friction distribution along the buried depth of the center, side, and corner piles for the 16 group piles under vertical loading in the 4*D* spacing condition is presented in Fig. 7. The overall trend of the lateral friction is an initial increase followed by a decrease. In the early stages of loading, the lateral friction in the upper portion of the long piles is not fully utilized. As the load increases, the lateral friction in the upper portion of the long piles gradually increases until it approaches its limit, at which point the lateral friction in the middle and upper portions of the long piles is fully utilized. At the working load ($Q_u/2$) for the long and short pile group foundations, the lateral friction of the short pile is 16 kPa, which is greater than that of the long pile. This indicates that at the working load, the lateral friction of the short pile is utilized before the long pile. Under the working load ($Q_u/2$), the ratio of pile-top reaction force to ultimate load was 0.41 for center piles, 0.46 for corner piles, and 0.47 for side piles. This indicates a greater contribution from short piles at lower load levels, with the influence of long piles increasing proportionally as the load increases. At ultimate bearing capacity, a greater proportion of the load was borne by the long piles compared to the short piles.

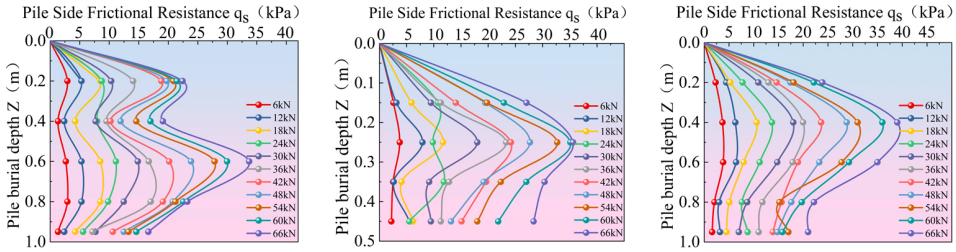

Fig. 7. Pile side friction resistance under 4*D* pile spacing: (a) 4# Center pile (long pile); (b) 7# Side pile (short pile); (c) 8# Corner pile (long pile)

A comparison of the characteristics and load-bearing characteristics of Table 2 long-short pile groups and equal-length pile groups is presented in Table 2, using the 4*D* spacing condition as an example. Table 2 indicates that increasing the length of selected piles within a group pile foundation leads to improved bearing capacity and reduced settlement. Moreover, appropriately increased pile length resulted in a slight reduction of the group pile effect coefficient.

Table 2. Comparison between long and short piles and equal-length group piles

Working condition	Ultimate bearing capacity of the group pile foundation (kN)	Group pile effect coefficient	Group pile settlement (mm)
1200 mm Equal-length pile group	83	0.80	6.1
600 mm Equal-length pile group	47	0.813	10.8
Combined long-short pile group	66	0.825	8.5

The axial force distribution curves along the pile embedment depth for center, edge, and corner piles in a 16-pile group with a 6*D* spacing are presented in Fig. 8. The bearing capacity of each pile in the group exhibits an increase when the pile spacing is expanded from 4*D* to 6*D*. Consequently, the pile group efficiency factor also increases from 0.825 for a pile spacing of 4*D* to 0.953 for a pile spacing of 6*D*. Increasing the pile spacing reduces the mutual influence of additional stresses generated by individual piles, leading to a significant improvement in the group's overall bearing capacity. The ultimate bearing capacity of the pile group increases from 66 kN to 77 kN as a result of the wider spacing. Under the working load (Q_u/2) and 6*D* spacing condition, the ratio of pile-top reaction force to ultimate load was 0.54 for both center and side piles and 0.49 for corner piles. These ratios indicate a substantial increase in bearing capacity for all piles. compared to the 4*D* pile spacing. A positive correlation exists between pile spacing and the group pile effect coefficient, with wider spacing resulting in a higher coefficient and an increased bearing capacity.

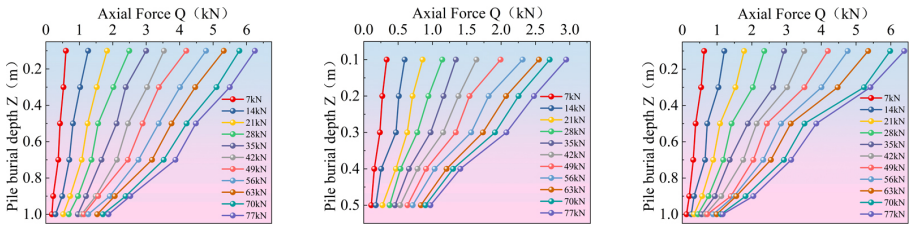

(a) (b) (c)

Fig. 8. Axial force of the pile under 6*D* work conditions: (a) 4# Center pile (long pile); (b) 7# Side pile (short pile); (c) 8# Corner pile (long pile)

The distribution curves of lateral friction resistance along the pile body for 16 group piles under vertical loading with a pile spacing of 6*D* are shown in Fig. 9. Increasing the pile spacing from 4*D* to 6*D* results in more fully mobilized lateral friction forces along the pile shaft. Additionally, this change in spacing reduces the interaction between foundation piles.

This behavior arises because the majority of the load in friction-type group piles is transferred through lateral resistance along the pile shaft. Furthermore, interactions between the pile, soil, and adjacent piles exist, and pile spacing directly influences the mobilization of lateral resistance and the superposition of these additional stresses. Smaller pile spacing leads to larger vertical soil displacements between piles, particularly as the influence of neighboring piles becomes more pronounced. Conversely, larger pile spacing decreases the relative displacement between piles and soil, reducing the overall impact on soil behavior. Increasing the pile spacing to 6*D* allows for the more complete mobilization of the lateral resistance of each pile, leading to a significant improvement in the bearing capacity of the group pile foundation.

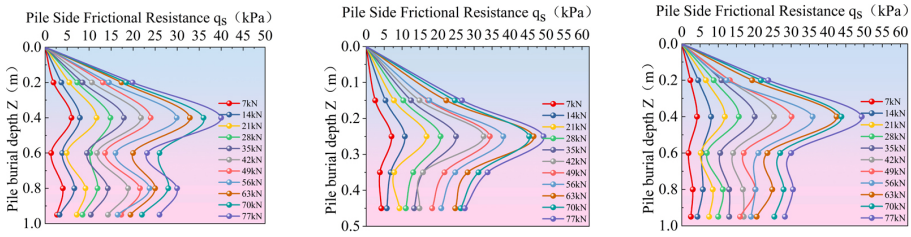

(a) (b) (c)

Fig. 9. Pile side friction resistance under 6*D* pile spacing: (a) 4# Center pile (long pile); (b) 7# Side pile (short pile); (c) 8# Corner pile (long pile)

4.2. Analysis of variable pile type experimental results

The axial force distribution curves along the pile embedment depth for center, edge, and corner piles in a triangular 16-pile group are presented in Fig. 10. The pile group arranged in a triangular pattern exhibits a 16% increase in bearing capacity compared to the foundation pile type. Furthermore, the bearing capacity of individual piles within the triangular pile group has also been enhanced. These findings indicate that a triangular pile arrangement is capable of supporting greater loads. For the triangular pile arrangement under the working load ($Q_u/2$), the ratios of pile head reaction force to ultimate load were 0.49 for the center pile and 0.52 for both corner and edge piles. Compared to the foundation pile arrangement, the corner and edge piles exhibit a noticeable increase in bearing capacity Compared to the foundation pile arrangement, the triangular arrangement minimizes the mutual interaction between adjacent piles.

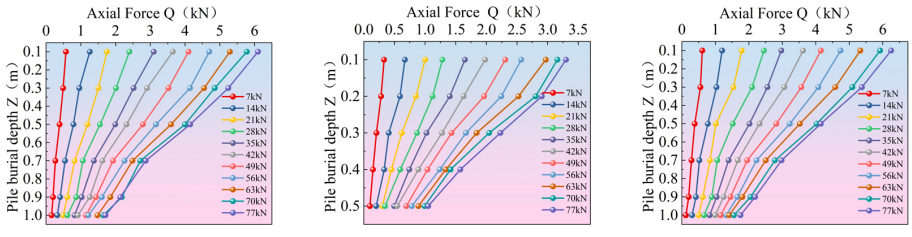

(a) (b) (c)

Fig. 10. Axial force of the plum blossom pile: (a) 2# Center pile (long pile); (b) 5# Side pile (short pile); (c) 6# Corner pile (long pile)

The lateral frictional resistance distribution curves along the pile embedment depth for center, edge, and corner piles in a triangular 16-pile group are shown in Fig. 11. The triangular arrangement exhibits a more complete mobilization of lateral frictional resistance in the corner, edge, and center piles compared to the foundation pile arrangement. Furthermore, the peak lateral frictional resistance in the triangular arrangement occurs at the mid-section of the pile, unlike the foundation pile arrangement where it is concentrated in the upper mid-section. In certain cases, the short piles display higher lateral frictional resistance than the long piles. This phenomenon might be attributed to the presence of custom-made settlement markers installed along the sides of the long piles. The manual compaction process might have failed to achieve optimal compaction density around the long piles, potentially hindering the full mobilization of lateral frictional resistance. The pile group efficiency factor for this pile type is 0.94, representing a modest improvement compared to the foundation pile arrangement.

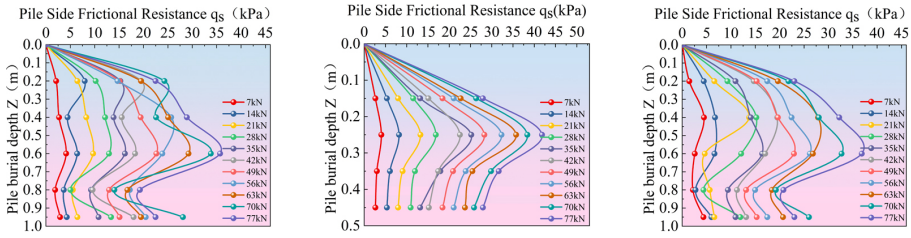

(a) (b) (c)

Fig. 11. Plum blossom pile arrangement pile side friction resistance: (a) 2# Center pile (long pile); (b) 5# Side pile (short pile); (c) 6# Corner pile (long pile)

4.3. Analysis of variable pile number experimental results

The axial force distribution curves along the pile embedment depth for the center, edge, and corner piles in a 16-pile group are presented in Fig. 12. In this cases, the axial force decreases rapidly in the upper mid-section of the pile and at a slower rate in the lower section. Furthermore, altering the number of piles resulted in a 20% reduction in the bearing capacity of the pile group foundation compared to the foundation pile arrangement.

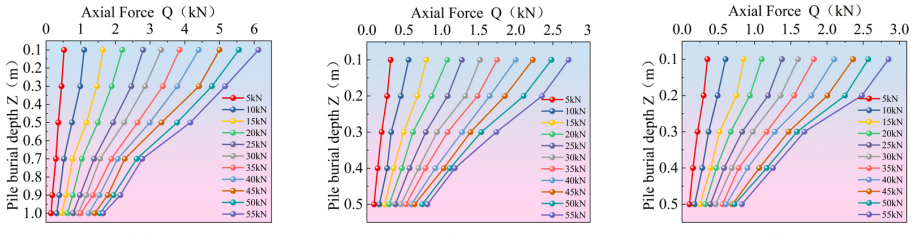

(a) (b) (c)

Fig. 12. Axial force of the pile under the condition of variable pile number: (a) 8# Center pile (long pile); (b) 5# Side pile (short pile); (c) 7# Corner pile (short pile)

Under working load, the short piles primarily contribute to the bearing capacity, while the long piles play a role in controlling settlement. However, under ultimate load, the axial force mobilized by the long piles significantly exceeds that of the short piles. Therefore, reducing the number of long piles in the combined long and short pile foundation is the primary reason for the decline in the group foundation's bearing capacity.

As observed in Fig. 13, the lateral frictional resistance in this arrangement generally increases with increasing pile embedment depth before eventually decreasing. Furthermore, the lateral frictional resistance of the piles in this arrangement is most fully mobilized in the upper mid-section of the pile shaft. Under working load ($Q_u/2$), the ratio of the pile top reaction force to the ultimate load pile top reaction force is 0.43 for the center pile long pile and 0.5 for the corner pile short pile. The corresponding ratio for the edge pile short pile is 0.48. These findings indicate that under working load, the short piles in this pile arrangement mobilize their bearing capacity earlier than the long piles. The pile group efficiency factor for this arrangement is 0.80, slightly lower than the 0.825 observed in the foundation pile arrangement. Furthermore, experimental findings indicate that the settlement in this arrangement is larger than that observed in the foundation pile arrangement. This is attributed to the reduction in the number of long piles weakens the settlement control capacity of the combined long and short pile foundation.

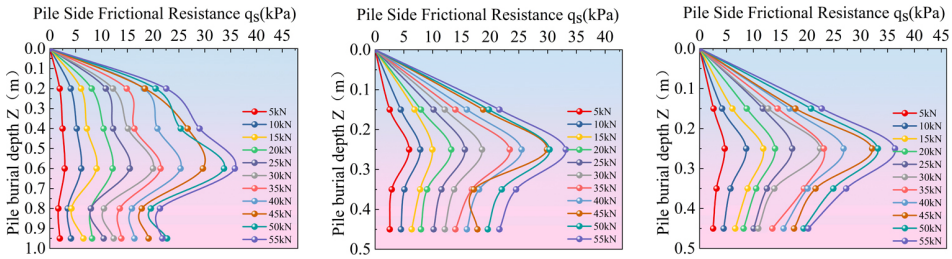

Fig. 13. Lateral friction resistance of the pile under the condition of variable pile number: (a) 8# Center pile (long pile); (b) 5# Side pile (short pile); (c) 7# Corner pile (short pile)

4.4. Analysis of variable pile length experimental results

The axial force distribution curves along the pile embedment depth are presented in Fig. 14 for center, edge, and corner piles in a 16-pile group. These curves are analyzed under varying pile lengths and vertical loading. Increasing the length of the long piles resulted in an 18.1% increase in the bearing capacity of the group foundation. The pile group efficiency factor for the arrangement with increased pile lengths is 0.87, a slight improvement compared to the baseline pile arrangement. This enhancement is attributed to the minimal or negligible interaction between the short piles and the lower portions of the long piles due to the increased length of a portion of the piles. A significant stress variation was observed at a pile embedment depth of 0.2 meters during the first load increment. Post-test analysis suggests that this anomaly may be attributed to the presence of loose soil at this depth due to insufficient compaction

after the installation of the earth pressure cell. This loose soil condition resulted in a lower soil density than the design specifications for the experiment, leading to a higher soil settlement rate compared to the pile settlement rate. This phenomenon is further evidenced by the presence of negative skin friction at the 0.2-meter depth in the subsequent lateral frictional resistance curves. However, this issue did not recur in subsequent load increments, corroborating the hypothesis regarding the cause of this error.

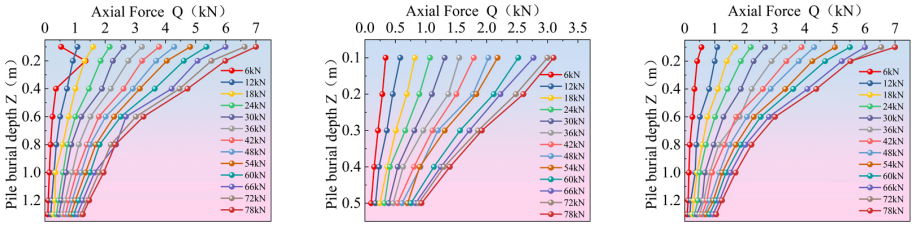

Fig. 14. Axial force of the pile under the condition of variable pile length: (a) 4# Center pile (long pile); (b) 7# Side pile (short pile); (c) 8# Corner pile (long pile)

The lateral friction distribution curves along the pile shaft depth, shown in Fig. 15, are presented for the central, edge, and corner piles of a 16-pile group. The figures demonstrate that the shaft friction of each pile is enhanced after increasing the pile length. As the pile embedment depth increases, the shaft friction generally exhibits a trend of first increasing and then decreasing, with the upper and middle portions of the pile shaft exhibiting the most effective shaft friction. Individual negative skin friction values were observed in the upper half of the central pile, while sudden increases and decreases in skin friction were observed at specific locations along the shaft of the shorter edge piles. As a consequence, during loading, the settlement rate of the surrounding soil may have exceeded the settlement rate of the pile, causing the observed fluctuations in skin friction. Compared to the baseline pile configuration, the variable pile length scenario resulted in increased shaft friction for the central pile and the long corner piles after pile length augmentation. However, the shaft friction of the shorter edge piles remained largely consistent with the baseline configuration.

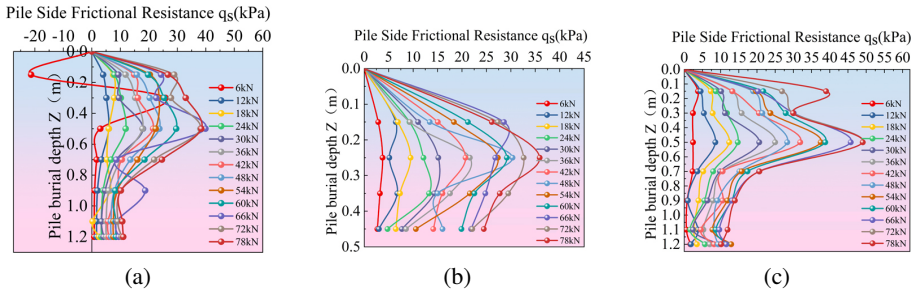

Fig. 15. Friction resistance of the pile under the condition of variable pile length: (a) 4# Center pile (long pile); (b) 7# Side pile (short pile); (c) 8# Corner pile (long pile)

5. Conclusions

1. In loess regions, the lateral frictional resistance of long and short piles in combined long and short pile foundations exhibits an asynchronous behavior, with alternating mobilization; comparisons with equivalent-length pile groups highlight the advantages of combined long and short pile foundations in terms of enhanced bearing capacity and reduced settlement.
2. Increasing pile spacing from 4*D* to 6*D* enhanced group pile bearing capacity by 16.7%, attributed to improved individual pile lateral frictional resistance mobilization and reduced pile-pile interaction. The group pile effect coefficient increased from 0.825 to 0.953.
3. Changing the pile arrangement from a basic circular to a staggered configuration significantly increased the individual pile bearing capacity. This change also resulted in a 16% improvement in overall group pile bearing capacity, with the group pile effect coefficient rising from 0.825 to 0.94.
4. Reducing the number of long piles resulted in a shift in the location of maximum lateral frictional resistance for the short piles from the mid-upper portion of the pile to the middle portion. This change, along with a reduction in the overall group pile-bearing capacity by approximately 20%. The group pile effect coefficient remained relatively consistent at 0.80.
5. Increasing long pile length enhanced group pile bearing capacity by 18.1%. This corresponded to an increase in the group pile effect coefficient from 0.825 to 0.87, suggesting improved lateral frictional resistance mobilization and load distribution.

Acknowledgements

This work was supported by the Natural Science Foundation of China (52068048).

References

[1] X. Huang and X. Yang, "Research progress of field water immersion test of collapsible loess", *Rock and Soil Mechanics*, vol. 34, no. S2, pp. 222–228, 2013, doi: 10.16285/j.rsm.2013.s2.068.

[2] Z. Li, C. Guan, M. Han, J. Jia, L. Liu, and W. Li, "Estimation of settlement in loess-filled subgrade with consideration of lateral deformation", *Arabian Journal for Science and Engineering*, vol. 47, no. 4, pp. 4713–4729, 2022, doi: 10.1007/s13369-021-06247-6.

[3] M. Yang and H. Yang, "Design Concept of Long and Short Pile Composite Pile Foundation and Analysis of Its Deformation Characteristics", *Journal of Civil Engineering*, vol. 38, no. 12, pp. 103–108, 2005.

[4] W. Wang, H. Yang, and M. Yang, "Analysis and evaluation of combined pile foundation with long and short piles", *Building Structure*, vol. 36, no. S1, pp. 836–839+846, 2006, doi: 10.19701/j.jzjg.2006.s1.205.

[5] S.H. Lee and C.K. Chung, "An experimental study of the interaction of vertically loaded pile groups in sand", *Canadian Geotechnical Journal*, vol. 42, no. 5, pp. 1485–1493, 2005, doi: 10.1139/t05-068.

[6] Q.Q. Zhang, S.M. Zhang, F.Y. Liang, Q. Zhang, and F. Xu, "Some observations of the influence factors on the response of pile groups", *KSCE Journal of Civil Engineering*, vol. 19, no. 6, pp. 1667–1674, 2015, doi: 10.1007/s12205-014-1550-7.

[7] L. Li and W. Gong, "Prediction of nonlinear vertical settlement of a pile group consisting of new and existing displacement piles in clay strata", *Soils and Foundations*, vol. 59, no. 5, pp. 1336–1348, 2019, doi: 10.1016/j.sandf.2019.06.001.

[8] L. Li, P. Zhang, Q. Long, H. Lei, and L. Zhao, "Study on the design scheme of pile group stiffness adjustment for a typical soft soil layer", *Journal of Railway Science and Engineering*, vol. 19, no. 5, pp. 1288–1297, 2022.

[9] F. Gao, X. Cheng, W. Wang, Q. Lv, and X. Cheng, "Experimental Study on the Bearing Characteristics of Rigid-Flexible Long-Short Pile Composite Foundations in Thick Collapsible Loess Areas", *KSCE Journal of Civil Engineering*, vol. 28, no. 5, pp. 1690–1701, 2024, doi: 10.1007/s12205-024-0052-5.

[10] S. Li, X. Ma, and Z. Tian, "Model test study on the reinforcement of loess foundation with long and short piles for high-speed railway", *Journal of the China Railway Society*, vol. 38, no. 10, pp. 78–84, 2016.

[11] M.F. Randolph and C.P. Wroth, "An analysis of the vertical deformation of pile groups", *Geotechnique*, vol. 29, no. 4, pp. 423–439, 1979, doi: 10.1680/geot.1979.29.4.423.

[12] M. Shi, X. Deng, and S. Liu, "Study on the interaction of "reinforcement and curtain" between pile groups", *Journal of Southeast University (Natural Science Edition)*, vol. 33, no. 3, pp. 343–346, 2003.

[13] T. Ma, Y. Zhu, and X. Yang, "Calculation of bearing capacity and deformation of composite pile foundation with long and short piles in loess areas", *Advances in Civil Engineering*, vol. 2020, art. no. 8829779, 2020, doi: 10.1155/2020/8829779.

[14] Y. Xiao and J. Wang, "Method of settlement calculation for underlying layer of soft soil composite foundation based on load transfer mechanism", *Archives of Civil Engineering*, vol. 70, no. 1, pp. 543–555, 2024, doi: 10.24425/ace.2024.148927.

[15] F.I. Shalabi, M.U. Saleem, H.J. Qureshi, M. Arifuzzaman, K. Khan, and M.M. Rahman, "3D FE analysis of bored pile-pile cap interaction in sandy soils under axial compression-parametric study", *Journal of Engineering Research*, vol. 11, no. 4, pp. 301–313, 2023, doi: 10.1016/j.jer.2023.07.004.

[16] A. Bhaduri and D. Choudhury, "Displacement-based finite element approach on analysing flexible combined pile–raft foundation in layered soil", *Canadian Geotechnical Journal*, vol. 60, no. 9, pp. 1370–1382, 2023, doi: 10.1139/cgj-2021-0310.

[17] H.C. Bernardes, R.P. da Cunha, A.J. da Cruz Junior, M.M. Sales, and J.F.R. Rebolledo, "Analysis of the geotechnical behavior of a piled raft in tropical lateritic soil based on long-term monitoring of columns, piles, and raft–soil interface", *Canadian Geotechnical Journal*, vol. 61, no. 4, pp. 627–648, 2024, doi: 10.1139/cgj-2022-0675.

[18] K. Danno, K. Isobe, and M. Kimura, "Pile group effect on end bearing capacity and settlement of pile foundation", *Japanese Geotechnical Journal*, vol. 3, no. 1, pp. 73–83, 2008.

[19] G. Kong, H. Gu, L. Zhou, and H. Peng, "Study on pile group effect coefficient of wedge-shaped pile with low cap widening", *Rock and Soil Mechanics*, vol. 37, no. S2, pp. 461–468, 2016, doi: 10.16285/j.rsm.2016.S2.060.

[20] JGJ94-2008 Technical code for building pile foundations. Ministry of Housing and Urban-Rural Development of the PRC, 2008.

[21] *Pile Foundation Engineering Handbook*. Beijing: Chinese Construction Industry Press, 1995.

Received: 2024-08-01, Revised: 2024-10-29